Food Chemistry: X 19 (2023) 100798

Contents lists available at ScienceDirect

Food Chemistry: X

journal homepage: www.sciencedirect.com/journal/food-chemistry-x

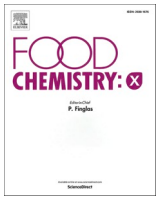

Rapid detection of *Salmonella* in food matrices by photonic PCR based on the photothermal effect of Fe_3O_4

Yuru Jiao, Zhen Zhang, Kaifei Wang, Hongyan Zhang *, Jianxin Gao *

Shandong Provincial Key Laboratory of Animal Resistance Biology, Key Laboratory of Food Nutrition and Safety of Shandong Normal University, College of Life Science, Shandong Normal University, Jinan 250014, PR China

ARTICLE INFO

Keywords:
Photonic PCR
Fe_3O_4
Salmonella typhimurium
Rapid detection
Food

ABSTRACT

Salmonella causes most deaths from diarrheal disease worldwide. Therefore, *Salmonella* must be accurately and quickly detected, even in complex food matrices, which is difficult to achieve using conventional culture methods. Here we propose a novel photonic polymerase chain reaction (PCR) method based on ferroferric oxide (Fe_3O_4) for the detection of *Salmonella typhimurium* in complex samples. Owing to the great photothermal conversion performance of Fe_3O_4, rapid thermal cycling could be accomplished. Our optimized photonic PCR system specifically detected *Salmonella typhimurium* in complex food matrices within 50 min. Quantitative data showed a limit of detection up to 10^2 CFU/mL in food samples. This method is suitable for the detection of all pathogenic microorganisms and is universal.

1. Introduction

Pathogenic bacteria are the main cause of morbidity and death worldwide (Kim, Jo, Mun, Noh & Kim, 2018). According to the World Health Organization, almost 76 million foodborne disease cases were reported each year, leading to 5000 deaths (Kim et al., 2018; Painter et al., 2013). *Salmonella* is a frequent cause of foodborne disease outbreaks and is a considerable public health concern in both developing and developed countries (Kirk et al., 2015). Over 75% of *Salmonella* outbreaks are caused by contaminated chicken, eggs, pork, and vegetables, so detecting bacteria in food using reliable methods of detection remains a critical public health need (Kang et al., 2021; Vinayaka et al., 2019).

Salmonella is traditionally detected by pre-enrichment, selective enrichment, time consuming isolation on selective agar plates, and then complicated serological and biochemical testing (van der Zee, 1994). This approach is complex, lengthy, and requires microbiological laboratory conditions, far from the practical need for timely and accurate detection. More recently, nucleic acid amplification has revolutionized the determination of pathogenic bacteria and viruses, especially polymerase chain reaction (PCR) (Kaminski, Abudayyeh, Gootenberg, Zhang & Collins, 2021; Lee, Park, Kim, Kwon, Rho & Jun 2019; Paul, Ostermann & Wei, 2020). However, conventional PCR uses expensive instruments, which are not always available in resource-poor settings and do not satisfy the demand for real-time rapid screening of large numbers of samples (Almassian, Cockrell & Nelson, 2013). To solve these problems, a PCR method using the photothermal effect of a nanomaterial was reported, termed photonic PCR (Kim, Kim, Park & Jon, 2017; You et al., 2020).

Ultrafast photonic PCR uses plasmonic photothermal conversion of a nanomaterial realized by photon-electron–phonon coupling on photothermal nanomaterials. Photothermal nanomaterials can therefore be used as efficient photothermal converters, allowing PCR to be completed in a shorter time (You et al., 2020). In early designs, a thin gold film was used as a photothermal source, but this did not produce the uniformity of temperature required for the PCR reaction (Son et al., 2015). To overcome the problem of temperature control, an optical cavity composed of two thin gold films was developed, and gold nanorods and bipyramids were added into the PCR reaction system as a photothermal converter (Kim et al., 2017; Lee et al., 2017; Son et al., 2016). Later, Jiang et al. and Wu et al. improved photonic PCR by coating ferroferric oxide (Fe_3O_4) with nanomaterials, exploiting the magnetic effect of Fe_3O_4 to separate the nanomaterials from the reaction solution for easy reaction visualization (Jiang et al., 2021; Wu et al., 2021). Most of these photonic PCR studies directly extracted DNA molecules as templates for detection (Jiang et al., 2021; Lee, Lee, Kim, Kim & Kim, 2022; Lee et al., 2020; Wu et al., 2021; You et al., 2021). Then, Cho et al. reported that photonic PCR can also detect bacteria directly, but only in simple

* Corresponding authors.
E-mail addresses: zhanghongyan@sdnu.edu.cn (H. Zhang), jxgao@sdnu.edu.cn (J. Gao).

https://doi.org/10.1016/j.fochx.2023.100798
Received 19 February 2023; Received in revised form 25 June 2023; Accepted 13 July 2023
Available online 19 July 2023

substrates such as urine (Cho et al., 2019). To date, to our best knowledge, there has been no report of photonic PCR applied to the detection of bacteria in complex substrates. Food substrates such as sugars, proteins, and lipids can affect the detection. In some cases, the need for samples to be pretreated could make the entire detection process more expensive and more complicated (Klein, Breuch, Reinmüller, Engelhard & Kaul, 2021; Zelada-Guillén, Bhosale, Riu & Rius, 2010). Since food samples are complex and heterogeneous systems, bacteria detection in food samples usually requires complex pretreatment, and bacterial isolation and enrichment with DNA amplification cannot be integrated into a single step (Wang, Cai, Gao, Yuan & Yue, 2020). Therefore, the rapid detection of bacteria in complex matrices without pretreatment would be a major breakthrough in rapid assays based on nucleic acid amplification.

In this paper, a novel photonic PCR system using the photothermal effect of Fe_3O_4 for the detection of pathogenic bacteria in food matrices was presented (Scheme 1). Magnetic Fe_3O_4 nanoparticles were selected as the photothermal converter, exploiting its magnetic property to separate and enrich bacteria and its photothermal property for photonic PCR. This allowed us to detect bacteria in a complex matrix and complete enrichment and amplification in one step without complex preprocessing, greatly reducing time and cost. The photothermal effect of magnetic Fe_3O_4 nanoparticles under 808 nm laser irradiation was used to achieve fast thermal cycling (40 thermal cycles in under 50 min), with the temperature of PCR reagents controlled by adjusting the laser switch (Fouad, El-Said & Mohamed, 2015). Anti-*Salmonella typhimurium* antibodies were conjugated to the magnetic nanoparticles and used to capture pathogenic bacteria from the food matrix, while the magnetism of the nanoparticles was used for separation and enrichment. This approach exploited not only the magnetism of Fe_3O_4 nanoparticles but also their photothermal property. Quantitative detection of target bacteria was achieved by the fluorescence of SYBR Green I, which interacted with final amplified product, double-stranded DNA (dsDNA), to produce fluorescence emission peaks of different intensities at 520 nm (Dragan et al., 2012; Wang, Ma, Li & Wu, 2019). The detection limit of the new method was 10^2 CFU/mL for *Salmonella typhimurium*. Our new photonic PCR system shows great potential for food safety monitoring.

2. Material and methods

2.1. Materials and reagents

Salmonella typhimurium (ATCC 14028), *Escherichia coli O157:H7* (ATCC 10907), *Listeria monocytogenes* (ATCC 23929), *Staphylococcus aureus* (CMCC 26001) and *Salmonella enteritidis* (ATCC 13076) were obtained from the National Center for Medical Culture Collections (CMCC) (Beijing, China). Monodispersed magnetite microspheres (200–300 nm) were purchased from Base Line Chromtech Research Center (Tianjin, China). The rabbit anti-*Salmonella typhimurium* antibody was acquired from Boorson biological Co., Ltd. (Beijing, China). Agar powder was acquired from Qingdao Hope Bio-Technology Co. Ltd. (Qingdao, China). Mineral oil was purchased from Sigma-Aldrich, Inc. (Shanghai, China). Bovine serum albumin (BSA), DNA Ladder and SYBR Green I (10000 ×) dye were obtained from Solarbio Biological Technology Co. Ltd. (Beijing, China). Nutrient broth (NB) was purchased from Beijing Aoboxing Bio-technology Co. Ltd. (Beijing, China). Ultra gelred (10000 ×) and 2 × rapid Taq master mix were purchased from Vazyme Biotech Co. Ltd. (Nanjing, China). Primers were ordered from

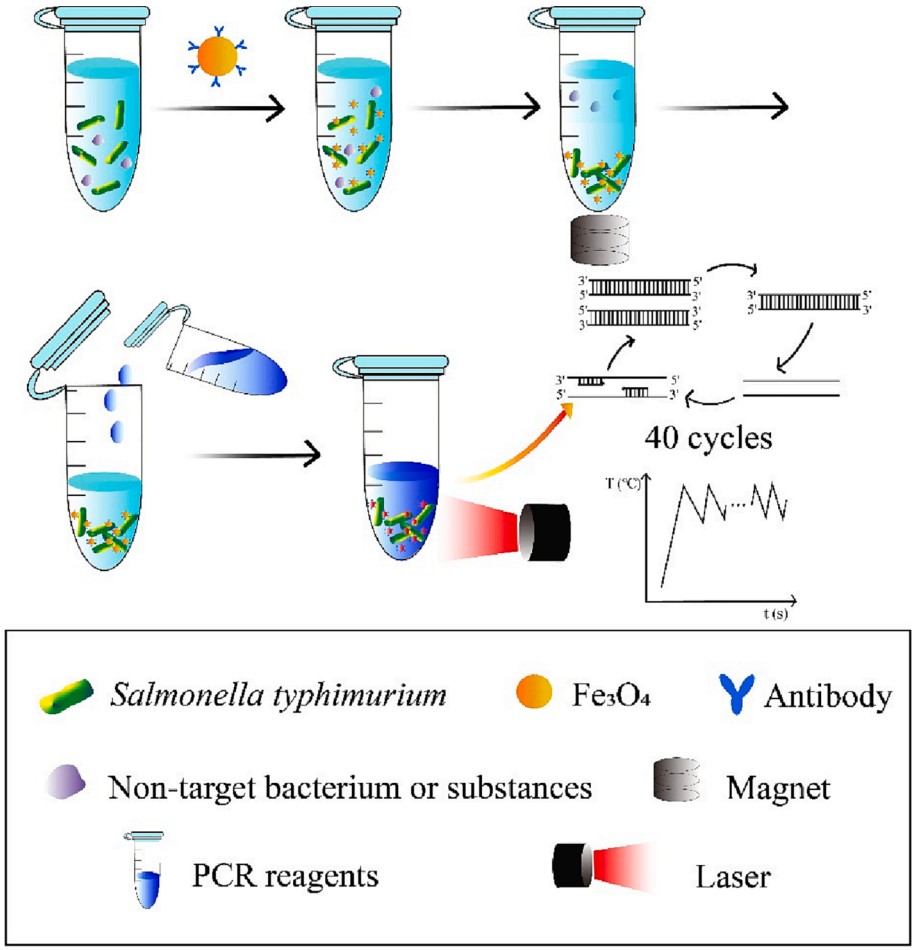

Scheme 1. Schematic illustration of the photonic PCR method based on the photothermal effect of Fe_3O_4.

Tsingke Biotechnology Co. Ltd. (Beijing, China). Milk, egg, pork and grape juice were obtained from a local supermarket (Jinan, China). The tap water used in validation experiments was collected from the laboratory tap. All laboratory experiments used ultrapure water.

2.2. Equipment

Magnetic separation racks were acquired from Jinan Chengsen Biotechnology Co. Ltd. (Jinan, China). The ADR-1860 near-infrared (IR) laser (808 nm) was used for irradiation and was acquired from Shanghai Xilong Photoelectric Technology Co, Ltd. (Shanghai, China). The thermal sensor (Fotric 225) for recording temperature changes was purchased from Fotric Precision Instruments (Shanghai, China). Fluorescence spectrophotometer was used for measuring the fluorescence intensity of PCR product and was acquired from Hitachi, Ltd. (Tokyo, Japan).

2.3. Bacterial culture

Bacteria were cultured as same as literature with slight modifications, pure bacterial colonies were cultured in NB liquid medium overnight at 37℃, 200 rpm (Du S., Wang, Liu, Xu & Zhang, 2019; Du, Lu, Gao, Ge, Xu & Zhang, 2020; Lu et al., 2022). The concentration of *Salmonella typhimurium* was calculated by the classical plate colony counting method. The collected bacterial liquid (5 mL) was diluted in a gradient, and then 200 μL of the bacterial solution from each dilution was evenly spread on the solid medium and colonies counted after culturing at 37℃ for 16 h.

2.4. Calculation of photothermal conversion efficiency

Photothermal conversion efficiency (η) of magnetic Fe_3O_4 nanoparticles was measured according to the following equation (Ren et al., 2015):

$$\eta = \frac{hA\Delta T_{max} - Q_s}{I\left(1 - 10^{-A_\lambda}\right)}$$

η: photothermal conversion efficiency;
I: laser power;
A_λ: absorbance of Fe_3O_4 magnetic nanoparticle at 808 nm;
h: heat transfer coefficient;
A: surface area of the container;
ΔT_{max}: maximum temperature change of the Fe_3O_4 magnetic nanoparticle;
Q_s: heat associated with the light absorbance of the solvent;
For pure water heating, the heat input equals the heat output at the highest steady state temperature, so the equation may be written as:

$$Q_s = Q_{loss} = hA\Delta T_{max,H_2O}$$

Where $\Delta T_{max,H_2O}$ is the maximum temperature change of water.

2.5. Preparation of immune-Fe_3O_4 complexes

The antibodies (50 μL, 10 μg/mL) were added dropwise into 50 μL magnetic Fe_3O_4 nanoparticles (5.0 mg/mL) and incubated in a low-speed shaker at 25℃ for 1 h. Finally, BSA (100 μL, 8% w/v) was added into the immune-Fe_3O_4 complex solution, followed by incubation for 2 h at 25℃ to block the active site and prevent the enzyme from adsorbing to the composite. After cleaning, complexes were redissolved in ultrapure water to the required concentrations (Lu et al., 2022).

2.6. Capture of pathogenic bacteria

Immune-Fe_3O_4 complexes (50 μL, 5.0 mg/mL) were added into 50 μL ultrapure water or samples containing *Salmonella typhimurium* and incubated in a low-speed shaker at 25℃ for 1 h to ensure that the target bacteria were captured on the immune-Fe_3O_4 complexes (Zhang, Wang, Han, Du, Yu & Zhang, 2018).

2.7. Detection of Salmonella typhimurium by photonic PCR

The primers used to amplify *Salmonella typhimurium* DNA were: the forward (5′-AGCGT ACTGG AAAGG GAAAG-3′) and reverse (5′-ATACC GCCAA TAAAG TTCAC AAAG-3′). The *Salmonella*-specific *invA* primers were designed to amplify a 116 bp sequence (Kasturi & Drgon, 2017). All pathogenic serotypes of *Salmonella* described thus far contain the *invA* gene, whose product plays a critical role in the ability of organisms to invade mammalian cells and subsequently cause disease (González-Escalona et al., 2009). Genomic *Salmonella typhimurium* DNA was used as a template. Light spots completely covered the bottom of eppendorf tube, including PCR reagents and Fe_3O_4 magnetic nanoparticles, during near-infrared laser irradiation. The PCR reagents for this method were: 12.5 μL of 2 × rapid Taq master mix, 1 μL each of forward and reverse primers, sterile ultrapure water to a total volume of 25 μL. Mineral oil (3 μL) was used to reduce the evaporation of water during photonic PCR (Kim et al., 2017). The thermal sensor recorded changes in temperature. Finally, the number of *Salmonella typhimurium* was estimated by measuring the fluorescence intensity of SYBR Green I interacted into the photonic PCR product. 3% agarose gel electrophoresis was carried out to further confirm PCR amplification. The selectivity of detection for *Salmonella typhimurium* was compared with other foodborne pathogenic bacteria.

2.8. Detection of Salmonella typhimurium in food samples

To detect *Salmonella typhimurium* in tap water, bacteria were first removed from the tap water. Then, multiple concentrations of *Salmonella typhimurium* suspension were centrifuged at 6000 rpm for 10 min (Lu et al., 2022). After removing the supernatant, the sediment was dissolved with sterile tap water, after which *Salmonella typhimurium* was captured using immune-Fe_3O_4 complexes in real samples. The following operations were the same as in Section 2.7 *Detection of Salmonella typhimurium by photonic PCR*.

For other samples, egg white (1 g) or pork (1 g) were mixed with 9 mL of ultrapure water and homogenized thoroughly. After which the mixture was centrifuged for 10 min at 10,000 rpm to remove any solid impurities present in both the egg white and pork samples. Bacteria in the supernatant were removed using a filter (0.22 μm pore size). For milk and grape juice, the bacteria were removed directly through a 0.22-μm filter. To explore the effect of food matrix on *Salmonella typhimurium* detection, 1 mL food matrix solution was mixed with 1 mL bacterial solution, and the volume was brought to 10 mL with sterile ultrapure water (Vinayaka et al., 2019). The volume of spiked samples was adjusted with sterile ultrapure water to obtain different concentrations of *Salmonella typhimurium* (Du et al., 2020; Lu et al., 2022). Then, immune-Fe_3O_4 complexes were applied to capture *Salmonella typhimurium* from real samples. The following operations were the same as in Section 2.7 *Detection of Salmonella typhimurium by photonic PCR*.

3. Results and discussion

3.1. Optimization of photonic PCR reaction

We compared the nucleic acid amplification capability of a Fe_3O_4-based photonic PCR with that of a conventional PCR. Photonic PCR was dependent on many factors and the optimal reaction conditions were determined by varying temperature, heating time and Fe_3O_4 concentration. DNA from *Salmonella typhimurium* was used as template for photonic PCR by irradiating with a laser and monitoring the temperature with a thermal imager. To confirm that the amplification was complete, the collected photonic PCR products were subjected to

agarose gel electrophoresis to determine their size (Fig. 1). The optimization results of the number of thermal cycles were presented in Fig. 1 (a), with the band brightness increasing as the number of cycles increased and plateauing at 40 cycles. Agarose gel electrophoresis was chosen for the accuracy of the experimental results during the conditional optimization process.

The PCR temperature was monitored by thermal imaging of the tube, although there are previous reports that the internal temperature of the PCR tube is higher than that of the surface. Therefore, thermal imaging requires optimization for photonic PCR. As shown in Fig. 1(b), denaturation temperatures of 75–80 ℃ and 80–85 ℃ produced dimmer and brighter bands, respectively. Furthermore, incomplete denaturation at the lower temperature (75–80℃) produced primer dimers below the target band, while a higher temperature (85–90℃) inactivated the enzyme. Therefore, a denaturation temperature of 80–85℃ was chosen. Similarly, as shown in Fig. 1(c), with increasing denaturation time, the target band brightness gradually decreased. However, no target band was generated for a denaturation time of 0 s. Finally, a denaturation time of 5 s was chosen. Fig. 1(d) and (e) showed the brightest target band with an annealing time of 10 s, and this was the same at an annealing temperature of 50–55℃ and 55–60℃. Considering that a higher annealing temperature during cooling can save time, the annealing temperature of 55–60℃ was chosen. Therefore, the final optimal photonic PCR reaction conditions were a denaturation temperature of 82–85℃ for 5 s, an annealing temperature of 55–57℃ for 10 s, and an extension temperature of 60℃ for 2 s. The photonic PCR took only 48 min to run 40 cycles.

3.2. Characterization of properties of Fe_3O_4

Fe_3O_4, as a good photothermal material, is often combined with other materials to form multifunctional nanocomposites for photothermal therapy (Jing, Zhi, Wang, Liu, Shao & Meng, 2018; Wang, Li, Chen, Dong, Liang & Yu, 2020; Xiao et al., 2019). Magnetic Fe_3O_4 nanoparticles can rapidly heat up when irradiated by near-IR light. Based on the above equations, the η value of magnetic Fe_3O_4 nanoparticles was 26.6%. Compared with gold nanomaterials, Fe_3O_4 was more stable at continuous high temperature with equivalent photothermal properties (González-Rubio et al., 2017; Li et al., 2016; You et al., 2020). Applying them for the first time to the detection of pathogenic bacteria in food, magnetic Fe_3O_4 nanoparticles represent a promising photothermal conversion material.

We previously demonstrated that Fe_3O_4 nanoparticles show a better photothermal effect and non-specific adsorption at 200–300 nm than at 100–200 nm and 10 nm (Zhang et al., 2018). Therefore, 200–300-nm magnetic Fe_3O_4 nanoparticles were selected as the photothermal conversion material for photonic PCR. The magnetic microspheres used here have uniform particle size distribution, consistent settlement speed in the magnetic field, and ultra-paramagnetism (Zhang et al., 2018). Fig. S1 showed that the particle size of Fe_3O_4 was 200–300 nm and the immune-Fe_3O_4 complexes successfully captured *Salmonella typhimurium*.

Researchers have previously reported that increasing PCR efficiency is influenced by the concentration of heat-conductive nanomaterials (Kim et al., 2017). Thus, the effect of PCR was evaluated as a function of Fe_3O_4 concentration from 2 mg/mL to 12 mg/mL. Fig. 2 showed the temperature distribution in a 200 μL PCR tube. Thermal cycling was carried out as follows: the maximum temperature was nearly 85℃ (denaturation), the minimum temperature was nearly 55℃ (annealing), and the final temperature was nearly 60℃ (extension). Different Fe_3O_4 concentrations had different photothermal conversion abilities. At Fe_3O_4 concentrations between 2 and 10 mg/mL, the time required to achieve a thermal cycle decreased as the concentration increased but then increased again at a concentration of 12 mg/mL.

Agarose gel electrophoresis images obtained by photonic PCR with different Fe_3O_4 concentrations were shown in Fig. 2(b). At magnetic Fe_3O_4 nanoparticle concentrations of 2–10 mg/mL, the brightness of agarose gel electrophoresis increased with increasing concentrations of nanomaterials to plateau at 10 mg/mL.

3.3. Fe_3O_4-based thermal cycling of photonic PCR

The system consists of a thermal imager, 808 nm laser, and Fe_3O_4 nanomaterial. The PCR temperature can be modulated by adjusting the laser output power. The photonic PCR system can achieve ultrafast thermal cycles of three different temperatures for denaturation, annealing, and extension.

As shown in Fig. 3(c), the laser output power to achieve thermal cycles was first optimized. When the PCR solution reached 80–85 ℃ for 5 s, 55–60℃ for 10 s, and 60℃ for 2 s, the laser output power was 0.40 W, 0.13 W, and 0.20 W, respectively. Thermal imaging was shown in Fig. 3(d), the solution in the tube reached the required, uniformly distributed temperature. It took about 27 min for 10 mg/mL magnetic Fe_3O_4 nanoparticles to achieve 40 thermal cycles at a maximum temperature of 85℃. The average ramp rate for heating and cooling in 40 thermal cycles could calculate as follows:

$$Ramprateforheating(i) = (T_{MAX,i} - T_{MIN,i})/t_{heat,i}$$

$$Ramprateforcooling(i) = (T_{MAX,i} - T_{MIN,i}^{'})/t_{cool,i}$$

where $T_{MAX,i}$, $T_{MIN,i}$ and $T_{MIN,i}^{'}$ are respectively the highest tempera-

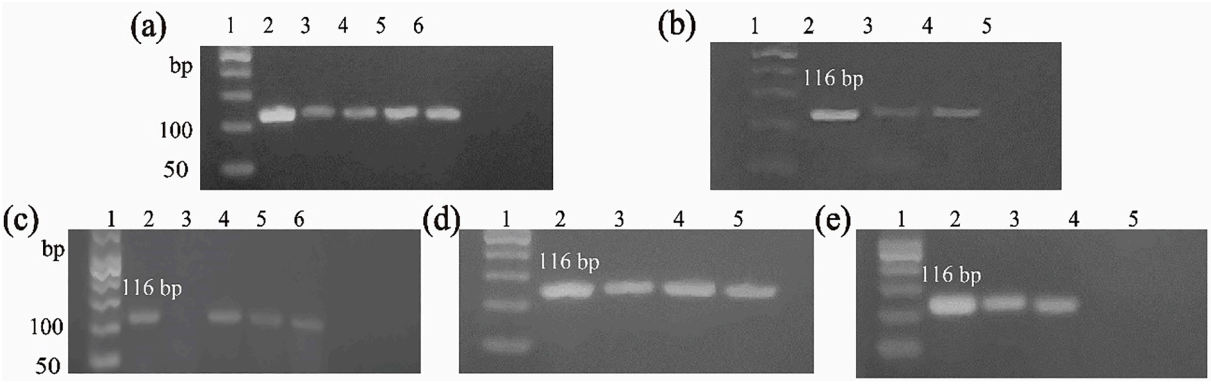

Fig. 1. Optimization of the number of thermal cycles (a). 1, DNA ladder; 2, conventional PCR, 40 cycles; 3–6, photonic PCR, 30, 35, 40 and 45 cycles. Optimization of the denaturation temperature (b). 1, DNA ladder; 2, conventional PCR, 95℃; 3–5, photonic PCR, 75–80℃, 80–85℃ and 85–90℃. Optimization of the time required for denaturation (c). 1, DNA ladder; 2, conventional PCR, 5 s; 3–6, photonic PCR, 0, 5, 10 and 15 s. Optimization of the time required for annealing (d). 1, DNA ladder; 2, conventional PCR, 10 s; 3–5, photonic PCR, 5, 10 and 15 s. Optimization of the annealing temperature (e). 1, DNA ladder; 2, conventional PCR, 60℃; 3–5, photonic PCR, 50–55℃, 55–60℃ and 60–65℃.

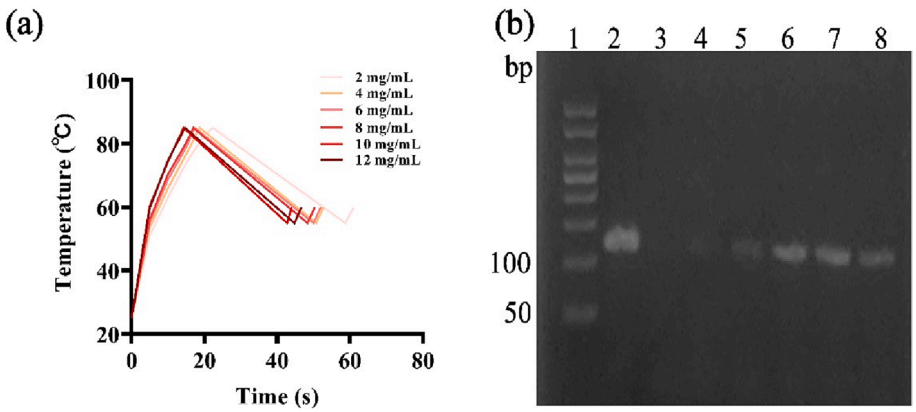

Fig. 2. The temperature profile of different concentrations of Fe_3O_4 for one thermocycle (a). Optimization of the concentrations of Fe_3O_4 by PCR (b). 1, DNA ladder; 2, conventional PCR, 10 mg/mL; 3–8, photonic PCR, 2–12 mg/mL.

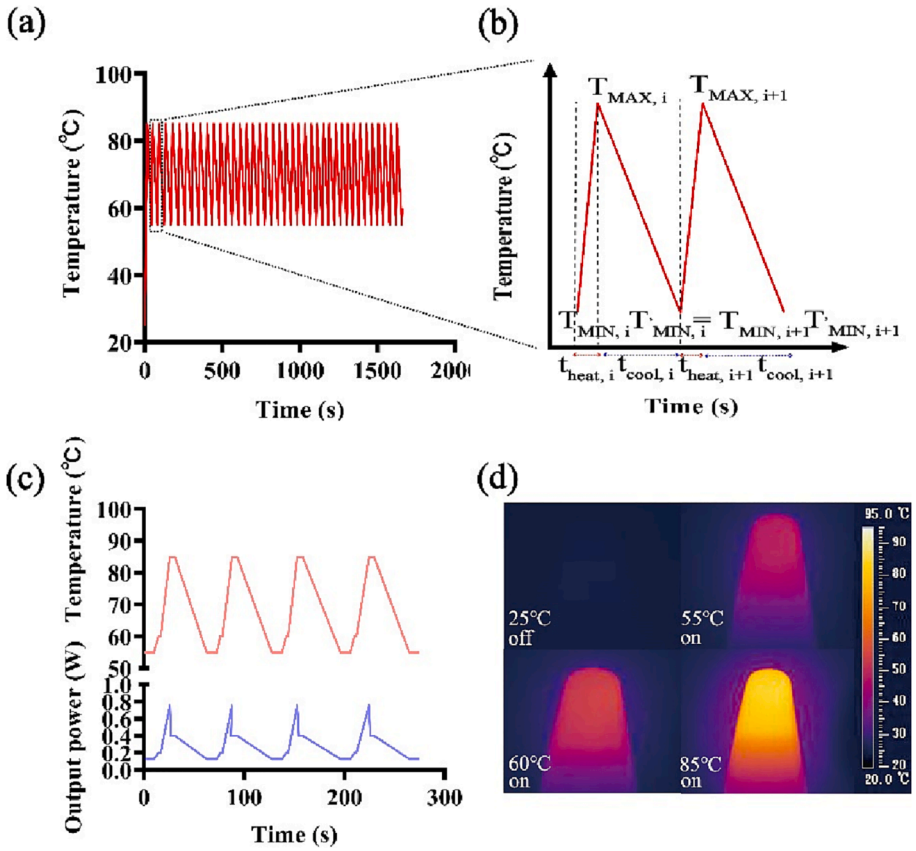

Fig. 3. The temperature profile for the 40 thermocycles (a). Characterization of ramp rate for heating and cooling (b). Temperature execution profile of the photothermal device (c). Thermal images of Fe_3O_4 solution upon infrared laser irradiation (d).

ture of cycle i, the lowest temperature of cycle i and i + 1, $t_{heat,i}$ and $t_{cool,i}$ are the time required for heating and cooling of cycle i. The average ramp rate for heating and cooling in 40 thermal cycles was calculated as 3.71℃/s and 0.90℃/s.

3.4. Accuracy assessment of the photonic PCR method

Salmonella typhimurium were first detected in ultrapure water. For quantitative detection, 2 × SYBR Green I dye was added to the PCR reaction mixtures after PCR amplification and the fluorescence signals measured. For reliability, the fluorescence intensity was measured by adding different volumes of SYBR Green I, which showed that increasing volumes of SYBR Green I enhanced the fluorescence intensity in the range of 2–12 μL, plateauing at 520 nm with 14 μL SYBR Green I (Fig. S2). As shown in Fig. 4(a), the concentration of *Salmonella typhimurium* was linear between 10^4 and 10^8 CFU/mL. A detection limit of 36 CFU/mL was calculated based on the equation: limit of detection = 3σ/k, where σ represents the standard deviation of the blank sample and k represents the slope of the analytical calibration curve. As shown in Fig. 4(b), the actual limit of detection was 100 CFU/mL. Repeatability was characterized by calculating the relative standard deviation of five repetitions (on one day), which was 3.99%.

The mean dose required for 50% probability of infection and illness ($InfD_{50}$ and $IllD_{50}$) was 4.33 × 10^3 and 1.25 × 10^8 CFU (Table S1). The

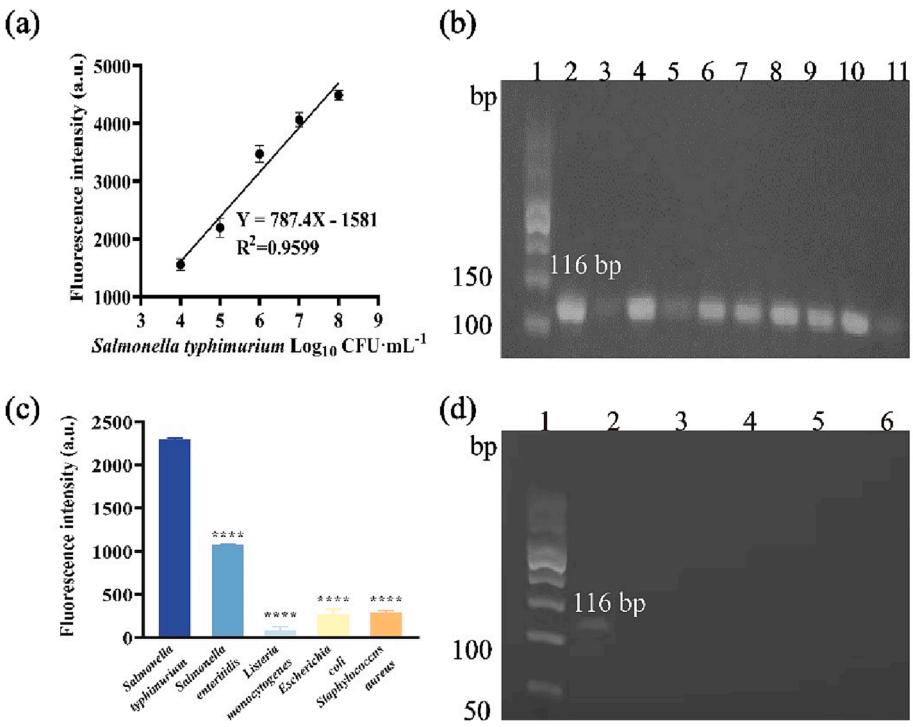

Fig. 4. Standard curve of photonic PCR for *Salmonella typhimurium* in ultrapure water (a). Photonic PCR in real samples (b). 1, DNA ladder; 2–3, tap water, 10^6 CFU/mL, 10^2 CFU/mL; 4–5, juice, 10^6 CFU/mL, 10^2 CFU/mL; 6–7, pork, 10^6 CFU/mL, 10^2 CFU/mL; 8–9, egg white, 10^6 CFU/mL, 10^2 CFU/mL; 10–11, milk, 10^6 CFU/mL, 10^2 CFU/mL. The fluorescence intensity of photonic PCR in the presence of different common bacteria (10^6 CFU/mL) (c). The selectivity of the detection was shown by agarose gel electrophoresis (d). 1, DNA ladder; 2–6, *Salmonella typhimurium*, *Salmonella enteritidis*, *Listeria monocytogenes*, *Escherichia coli*, *Staphylococcus aureus*.

detection limit of this established method was 10^2 CFU/mL, which can realize the detection of the mean dose. The flow-chart was shown in Fig. S3. Due to the 1% probability of infection and illness ($InfD_{01}$ and $IllD_{01}$), a lower dose was required, so the proposed method was less efficient against those concentrations.

To further evaluate detection in real samples, *Salmonella typhimurium* was measured in tap water, juice, pork, egg white, and milk spiked with various concentrations of target bacteria (10^5, 10^6, and 10^8 CFU/mL). Table 1 shows 82.9%~114% recoveries from all samples with relative standard deviations $\leq$ 4.51%. Due to the strong signal interference of fat and protein in milk, the recovery rate of milk spiked samples is slightly lower (Bai et al., 2020). It can be concluded that all these are beneficial to the development and application of photonic PCR assays for the detection of *Salmonella typhimurium* in real samples.

3.5. Selectivity assessment of photonic PCR

The selectivity of photonic PCR system was tested using other common bacteria (10^6 CFU/mL), including water as blank, *Salmonella typhimurium* as target. As shown in Fig. 4(c), the fluorescence intensities at 520 nm for *Salmonella typhimurium* peaked at 2299.4, but the fluorescence intensities of other non-targeted bacteria were all low. Photonic PCR had high selectivity for *Salmonella typhimurium*, due to the recognition specificity of the primers and antibodies.

Table 1
Spiked recoveries.

Samples	Spiked Log_{10} (CFU/mL)	Tested Log_{10} (CFU/mL)	Recovery (%)	CV (%)
Tap water	5.00	5.70	114	2.16
	6.00	6.70	111	2.94
	8.00	6.90	86.3	0.480
Juice	5.00	5.30	105	2.04
	6.00	6.10	111	1.88
	8.00	6.90	86.0	2.01
Pork	5.00	5.20	104	4.51
	6.00	5.00	82.9	0.840
	8.00	6.90	86.4	0.660
Egg white	5.30	5.90	110	2.52
	6.30	6.70	106	0.930
	8.30	7.70	92.4	0.710
Milk	5.40	5.10	94.1	0.810
	6.40	6.00	93.6	1.35
	8.40	7.50	88.8	1.70

CV = coefficient of variation.

3.6. Stability assessment

Photonic PCR relied on the photothermal conversion efficiency of Fe_3O_4. Since the storage stability of Fe_3O_4 was very important, the temperature change of Fe_3O_4 under different storage conditions was measured to judge its stability. Fig. S4(a) showed that Fe_3O_4 could be stored stably at 4℃ for at least half a year. Immune-Fe_3O_4 complexes stability mainly depended on the activity of anti-*Salmonella* antibodies on Fe_3O_4. As shown in Fig. S4(b) the antibodies-coated and BSA-blocked Fe_3O_4 was placed at 4℃ for 10 d, and then the detection efficiency of *Salmonella typhimurium* can be retained 80.3%.

3.7. Comparison of detection methods for Salmonella typhimurium

As shown in Table S2, we summarized five aspects of reported nanomaterial-based immunoassay methods for *Salmonella typhimurium*, including methods, nanomaterials, samples, linear range, and limit of detection. The advantages of photonic PCR over conventional PCR and real-time PCR methods are the lack of bulky instrumentation, low cost, and simplicity of operation. Although this is not the lowest detection limit of the method established in this paper, it is on the same order of magnitude as the other fast detection methods, and may meet the requirements for detection of the infection dose of *Salmonella typhimurium* outbreaks (10^5 CFU mL^{-1}). In summary, the established photonic PCR detection method can be sensitive and accurate for realizing the detection of *Salmonella typhimurium* in real samples, and has a good prospect for application.

4. Conclusions

In conclusion, an ultrafast photonic PCR system for detecting *Salmonella typhimurium* was established with a limit of detection of 10^2 CFU/mL. Our photonic PCR Fe_3O_4-based specifically detected *Salmonella typhimurium* in food matrices for the first time. The photonic PCR system contains Fe_3O_4 nanomaterial, a thermal imager, and a 808 nm laser, which allowed 40 rapid thermal cycles in under 50 min. This system enabled the rapid detection of bacteria in complex food samples without the need for expensive additional equipment and sophisticated preprocessing. Future developments will package the photonic PCR system into a small detection device that can display the measured fluorescence intensity through smart phones. This method is suitable for the detection of all pathogenic microorganisms and is universal.

CRediT authorship contribution statement

Yuru Jiao: Data curation, Investigation, Validation, Formal analysis, Writing – original draft. **Zhen Zhang:** Formal analysis, Validation, Investigation, Resources. **Kaifei Wang:** Formal analysis, Validation. **Hongyan Zhang:** Conceptualization, Methodology, Resources, Supervision, Project administration, Funding acquisition. **Jianxin Gao:** Conceptualization, Methodology, Formal analysis, Writing – review & editing.

Declaration of Competing Interest

The authors declare that they have no known competing financial interests or personal relationships that could have appeared to influence the work reported in this paper.

Data availability

The data that has been used is confidential.

Acknowledgements

This work was supported by the National Natural Science Foundation of China (grant number U22A20550, Key Program); and the Natural Science Foundation of Shandong Province (grant number ZR2020KC031, Key Program).

Appendix A. Supplementary data

Supplementary data to this article can be found online at https://doi.org/10.1016/j.fochx.2023.100798.

References

Almassian, D. R., Cockrell, L. M., & Nelson, W. M. (2013). Portable nucleic acid thermocyclers. *Chemical Society Reviews, 42*(22), 8769–8798. https://doi.org/10.1039/c3cs60144g

Bai, H., Bu, S., Wang, C., Ma, C., Li, Z., Hao, Z., … Han, Y. (2020). Sandwich immunoassay based on antimicrobial peptide-mediated nanocomposite pair for determination of *Escherichia coli* O157:H7 using personal glucose meter as readout. *Microchimica Acta, 187*(4), 220. https://doi.org/10.1007/s00604-020-4200-4

Cho, B., Lee, S. H., Song, J., Bhattacharjee, S., Feng, J., Hong, S., … Lee, L. P. (2019). Nanophotonic cell lysis and polymerase chain reaction with gravity-driven cell enrichment for rapid detection of pathogens. *ACS Nano, 13*(12), 13866–13874. https://doi.org/10.1021/acsnano.9b04685

Dragan, A. I., Pavlovic, R., McGivney, J. B., Casas-Finet, J. R., Bishop, E. S., Strouse, R. J., … Geddes, C. D. (2012). SYBR Green I: Fluorescence properties and interaction with DNA. *Journal of Fluorescence, 22*(4), 1189–1199. https://doi.org/10.1007/s10895-012-1059-8

Du, S., Wang, Y., Liu, Z., Xu, Z., & Zhang, H. (2019). A portable immune-thermometer assay based on the photothermal effect of graphene oxides for the rapid detection of *Salmonella typhimurium*. *Biosensors & Bioelectronics, 144*, Article 111670. https://doi.org/10.1016/j.bios.2019.111670

Du, S., Lu, Z., Gao, L., Ge, Y., Xu, X., & Zhang, H. (2020). *Salmonella typhimurium* detector based on the intrinsic peroxidase-like activity and photothermal effect of MoS_2. *Microchimica Acta, 187*(11). https://doi.org/10.1007/s00604-020-04600-4

Fouad, D. M., El-Said, W. A., & Mohamed, M. B. (2015). Spectroscopic characterization of magnetic Fe_3O_4@Au core shell nanoparticles. *Spectrochimica Acta Part A: Molecular and Biomolecular Spectroscopy, 140*, 392–397. https://doi.org/10.1016/j.saa.2014.12.097

González-Escalona, N., Hammack, T. S., Russell, M., Jacobson, A. P., De Jesús, A. J., Brown, E. W., & Lampel, K. A. (2009). Detection of live *Salmonella* sp. cells in produce by a TaqMan-based quantitative reverse transcriptase real-time PCR targeting *invA* mRNA. *Applied and Environmental Microbiology, 75*(11), 3714–3720. https://doi.org/10.1128/AEM.02686-08

González-Rubio, G., Díaz-Núñez, P., Rivera, A., Prada, A., Tardajos, G., González-Izquierdo, J., … Guerrero-Martínez, A. (2017). Femtosecond laser reshaping yields gold nanorods with ultranarrow surface plasmon resonances. *Science, 358*(6363), 640–644. https://doi.org/10.1126/science.aan8478

Jiang, K., Wu, J., Qiu, Y., Go, Y. Y., Ban, K., Park, H. J., & Lee, J. (2021). Plasmonic colorimetric PCR for rapid molecular diagnostic assays. *Sensors and Actuators B: Chemical, 337*, Article 129762. https://doi.org/10.1016/j.snb.2021.129762

Jing, X., Zhi, Z., Wang, D., Liu, J., Shao, Y., & Meng, L. (2018). Multifunctional nanoflowers for simultaneous multimodal imaging and high-sensitivity chemo-photothermal treatment. *Bioconjugate Chemistry, 29*(2), 559–570. https://doi.org/10.1021/acs.bioconjchem.8b00053

Kaminski, M. M., Abudayyeh, O. O., Gootenberg, J. S., Zhang, F., & Collins, J. J. (2021). CRISPR-based diagnostics. *Nature. Biomedical Engineering, 5*(7), 643–656. https://doi.org/10.1038/s41551-021-00760-7

Kang, B. H., Lee, Y., Yu, E. S., Na, H., Kang, M., Huh, H. J., & Jeong, K. H. (2021). Ultrafast and real-time nanoplasmonic on-chip polymerase chain reaction for rapid and quantitative molecular diagnostics. *ACS Nano, 15*(6), 10194–10202. https://doi.org/10.1021/acsnano.1c02154

Kasturi, K. N., & Drgon, T. (2017). Real-time PCR method for detection of *Salmonella* spp. in environmental samples. *Applied and Environmental Microbiology, 83*(14), e617–e644. https://doi.org/10.1128/AEM.00644-17

Kim, J., Kim, H., Park, J. H., & Jon, S. (2017). Gold nanorod-based photo-PCR system for one-step, rapid detection of bacteria. *Nanotheranostics, 1*(2), 178–185. https://doi.org/10.7150/ntno.18720

Kim, S. U., Jo, E., Mun, H., Noh, Y., & Kim, M. (2018). Ultrasensitive detection of *Escherichia coli* O157:H7 by immunomagnetic separation and selective filtration with nitroblue tetrazolium/5-Bromo-4-chloro-3-indolyl phosphate signal amplification. *Journal of Agricultural and Food Chemistry, 66*(19), 4941–4947. https://doi.org/10.1021/acs.jafc.8b00973

Kirk, M. D., Pires, S. M., Black, R. E., Caipo, M., Crump, J. A., Devleesschauwer, B., Döpfer, D., Fazil, A., Fischer-Walker, C. L., Hald, T., Hall, A. J., Keddy, K. H., Lake, R. J., Lanata, C. F., Torgerson, P. R., Havelaar, A. H., & Angulo, F. J. (2015). World health organization estimates of the global and regional disease burden of 22 foodborne bacterial, protozoal, and viral diseases, 2010: A data synthesis. *Plos Medicine, 12*(12), e1001921. https://doi.org/ 10.1371/journal.pmed.1001921.

Klein, D., Breuch, R., Reinmüller, J., Engelhard, C., & Kaul, P. (2021). Rapid detection and discrimination of food-related bacteria using IR-microspectroscopy in combination with multivariate statistical analysis. *Talanta, 232*, Article 122424. https://doi.org/10.1016/j.talanta.2021.122424

Lee, B., Lee, Y., Kim, S., Kim, K., & Kim, M. (2022). Rapid membrane-based photothermal PCR for disease detection. *Sensors and Actuators B: Chemical, 360*, Article 131554. https://doi.org/10.1016/j.snb.2022.131554

Lee, J. H., Cheglakov, Z., Yi, J., Cronin, T. M., Gibson, K. J., Tian, B., & Weizmann, Y. (2017). Plasmonic photothermal gold bipyramid nanoreactors for ultrafast real-time bioassays. *Journal of the American Chemical Society, 139*(24), 8054–8057. https://doi.org/10.1021/jacs.7b01779

Lee, S. H., Park, S. M., Kim, B. N., Kwon, O. S., Rho, W. Y., & Jun, B. H. (2019). Emerging ultrafast nucleic acid amplification technologies for next-generation molecular diagnostics. *Biosensors and Bioelectronics, 141*, Article 111448. https://doi.org/10.1016/j.bios.2019.111448

Lee, Y., Kang, B. H., Kang, M., Chung, D. R., Yi, G. S., Lee, L. P., & Jeong, K. H. (2020). Nanoplasmonic on-chip PCR for rapid precision molecular diagnostics. *ACS Applied Materials & Interfaces, 12*(11), 12533–12540. https://doi.org/10.1021/acsami.9b23591

Li, T., Chang, C., Chang, P., Chuang, Y., Huang, C., Su, W., & Shieh, D. (2016). Handheld energy-efficient magneto-optical real-time quantitative PCR device for target DNA enrichment and quantification. *NPG Asia Materials, 8*(6), e277.

Lu, Z., Liu, W., Cai, Y., Zhao, T., Cui, M., Zhang, H., & Du, S. (2022). *Salmonella typhimurium* strip based on the photothermal effect and catalytic color overlap of PB@Au nanocomposite. *Food Chemistry, 385*, Article 132649. https://doi.org/10.1016/j.foodchem.2022.132649

Painter, J. A., Hoekstra, R. M., Ayers, T., Tauxe, R. V., Braden, C. R., Angulo, F. J., & Griffin, P. M. (2013). Attribution of foodborne illnesses, hospitalizations, and deaths to food commodities by using outbreak data, United States, 1998–2008. *Emerging Infectious Diseases, 19*(3), 407–415. https://doi.org/10.3201/eid1903.111866

Paul, R., Ostermann, E., & Wei, Q. (2020). Advances in point-of-care nucleic acid extraction technologies for rapid diagnosis of human and plant diseases. *Biosensors and bioelectronics, 169*, Article 112592. https://doi.org/10.1016/j.bios.2020.112592

Ren, W., Yan, Y., Zeng, L., Shi, Z., Gong, A., Schaaf, P., … Wu, A. (2015). A Near Infrared Light Triggered Hydrogenated Black TiO_2 for Cancer Photothermal Therapy. *Advanced Healthcare Materials, 4*(10), 1526–1536. https://doi.org/10.1002/adhm.201500273

Son, J. H., Cho, B., Hong, S., Lee, S. H., Hoxha, O., Haack, A. J., & Lee, L. P. (2015). Ultrafast photonic PCR. *Light: Science & Applications, 4*(7), e280.

Son, J. H., Hong, S., Haack, A. J., Gustafson, L., Song, M., Hoxha, O., & Lee, L. P. (2016). Rapid optical cavity PCR. *Advanced Healthcare Materials, 5*(1), 167–174. https://doi.org/10.1002/adhm.201500708

van der Zee, H. (1994). Conventional methods for the detection and isolation of *Salmonella enteritidis*. *International Journal of Food Microbiology, 21*(1), 41–46. https://doi.org/10.1016/0168-1605(94)90198-8

Vinayaka, A. C., Ngo, T. A., Kant, K., Engelsmann, P., Dave, V. P., Shahbazi, M., … Bang, D. D. (2019). Rapid detection of *Salmonella enterica* in food samples by a novel approach with combination of sample concentration and direct PCR. *Biosensors and bioelectronics, 129*, 224–230. https://doi.org/10.1016/j.bios.2018.09.078

Wang, H., Ma, C., Li, Z., & Wu, K. (2019). An exonuclease-assisted fluorescence sensor for assaying alkaline phosphatase based on SYBR Green I. *Molecular and Cellular Probes, 45*, 26–30. https://doi.org/10.1016/j.mcp.2019.04.002

Wang, Y., Li, X., Chen, P., Dong, Y., Liang, G., & Yu, Y. (2020). Enzyme-instructed self-aggregation of Fe_3O_4 nanoparticles for enhanced MRIT2 imaging and photothermal therapy of tumors. *Nanoscale, 12*(3), 1886–1893. https://doi.org/10.1039/C9NR09235H

Wang, Z., Cai, R., Gao, Z., Yuan, Y., & Yue, T. (2020). Immunomagnetic separation: An effective pretreatment technology for isolation and enrichment in food microorganisms detection. *Comprehensive Reviews in Food Science and Food Safety, 19*(6), 3802–3824. https://doi.org/10.1111/1541-4337.12656

Wu, J., Jiang, K., Mi, H., Qiu, Y., Son, J., Park, H. J., … Lee, J. (2021). A rapid and sensitive fluorescence biosensor based on plasmonic PCR. *Nanoscale, 13*(15), 7348–7354. https://doi.org/10.1039/D1NR00102G

Xiao, L., Wu, Z., Zhang, J., Wang, G., Ma, Y., Ding, Y., … Zhang, Z. (2019). Synthesis, Photothermal Effect and Cytotoxicity of Fe_3O_4@Au Nanocomposites. *Journal of Nanoscience and Nanotechnology, 19*(5), 2467–2473. https://doi.org/10.1166/jnn.2019.16031

You, M., Jia, P., He, X., Wang, Z., Feng, S., Ren, Y., … Xu, F. (2021). Quantifying and adjusting plasmon-driven nano-localized temperature field around gold nanorods for nucleic acids amplification. *Small Methods, 5*(5), 2001254. https://doi.org/10.1002/smtd.202001254

You, M., Li, Z., Feng, S., Gao, B., Yao, C., Hu, J., & Xu, F. (2020). Ultrafast photonic PCR based on photothermal nanomaterials. *Trends in Biotechnology, 38*(6), 637–649. https://doi.org/10.1016/j.tibtech.2019.12.006

Zelada-Guillén, G. A., Bhosale, S. V., Riu, J., & Rius, F. X. (2010). Real-time potentiometric detection of bacteria in complex samples. *Analytical Chemistry, 82*(22), 9254–9260. https://doi.org/10.1021/ac101739b

Zhang, Z., Wang, Q., Han, L., Du, S., Yu, H., & Zhang, H. (2018). Rapid and sensitive detection of *Salmonella typhimurium* based on the photothermal effect of magnetic nanomaterials. *Sensors and Actuators B: Chemical, 268*, 188–194. https://doi.org/10.1016/j.snb.2018.04.043